



Efficient Degradation of Sulfamethoxazole by Diatomite-Supported Hydroxyl-Modified UIO-66 Photocatalyst after Calcination

Hui-Lai Liu ^{1,2}, Yu Zhang ^{1,2}, Xin-Xin Lv ^{1,2}, Min-Shu Cui ¹, Kang-Ping Cui ¹, Zheng-Liang Dai ³, Bei Wang ³, Rohan Weerasooriya ^{2,4} and Xing Chen ^{1,2,4,*}

¹ Key Laboratory of Nanominerals and Pollution Control of Higher Education Institutes, School of Resources and Environmental Engineering, Hefei University of Technology, Hefei 230009, China; 18255110208@163.com (H.-L.L.); 18691965261@163.com (Y.Z.); lvx1996@163.com (X.-X.L.); mcui@mail.ustc.edu.cn (M.-S.C.); cuikangping@hfut.edu.cn (K.-P.C.)

² Key Lab of Aerospace Structural Parts Forming Technology and Equipment of Anhui Province, Institute of Industry and Equipment Technology, Hefei University of Technology, Hefei 230009, China; rohan.we@nifs.ac.lk

³ Anqing Changhong Chemical Co., Ltd., Anqing 246002, China; 18256240803@163.com (Z.-L.D.); 13855694589@163.com (B.W.)

⁴ National Centre for Water Quality Research, National Institute of Fundamental Studies, Hantana, Kandy, Sri Lanka; rohan.we@nifs.ac.lk

* Correspondence: xingchen@hfut.edu.cn

Photoelectrochemical measurements

The photocurrent measurements were carried out on a CHI-760E electrochemical workstation (Chenhua Instrument, Shanghai, China) in a conventional three-electrode configuration with the sample modified ATO (20 mm * 50 mm) as the working electrode, Pt as the counter electrode, and Ag/AgCl as the reference electrode. The current measurement *i*-*t* curve was performed using an LED lamp (35 W) at 0.4 V bias voltage potential. An aqueous solution of 0.5 M Na₂SO₄ was used as the electrolyte.

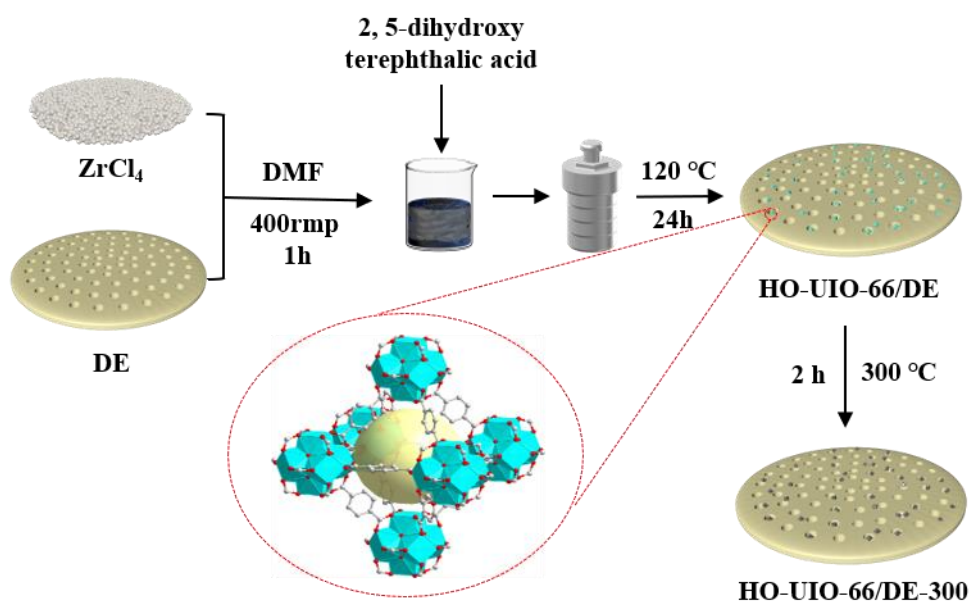


Figure S1. Schematic of the synthesis process of HO-UIO-66/DE-300.

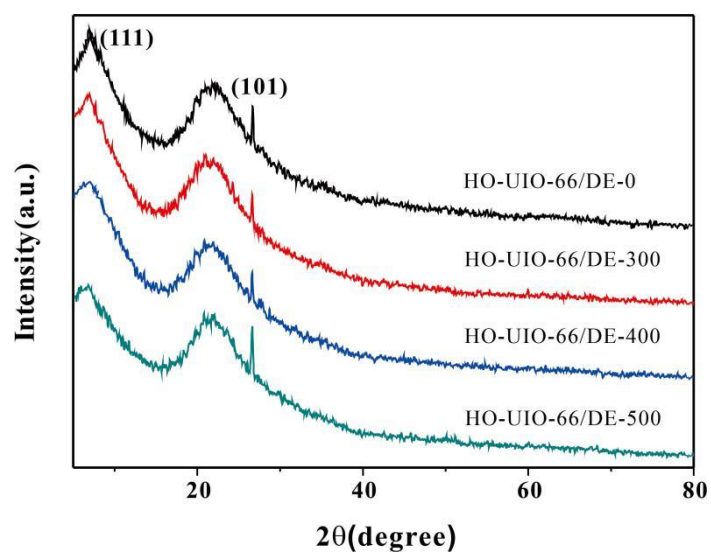


Figure S2. The XRD patterns of synthesized photocatalysts.

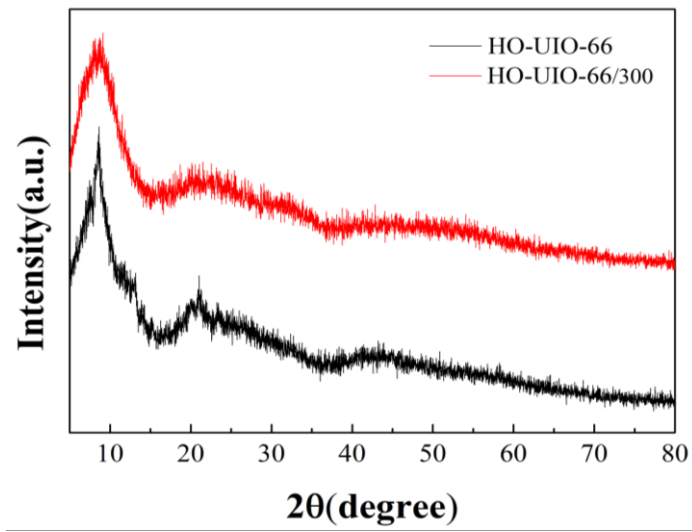


Figure S3. The XRD patterns of HO-UIO-66 and HO-UIO-66/300.

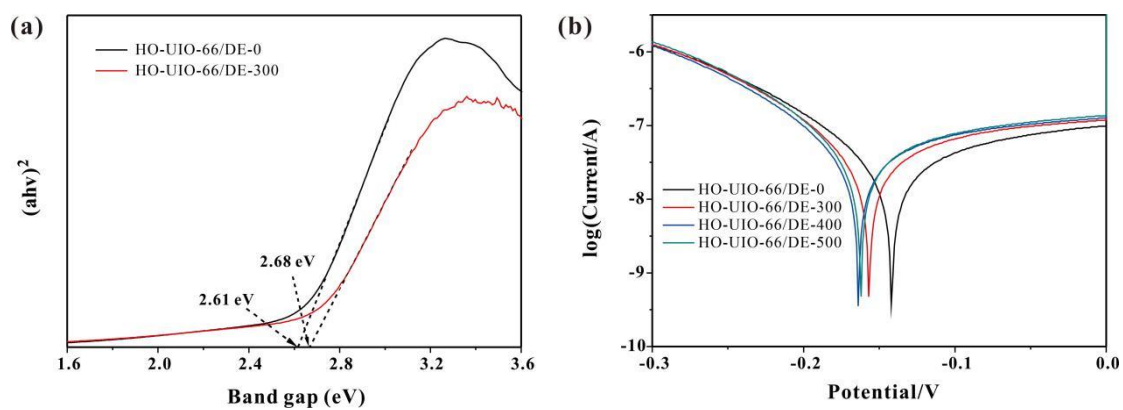


Figure S4. (a) Tauc plots of as-prepared catalysts and (b) Tafel polarization curves.

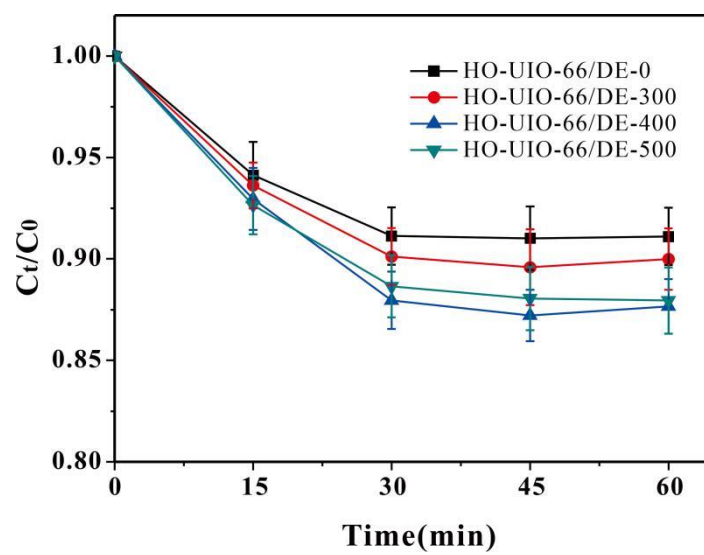


Figure S5. The effect of different catalysts on SMX adsorption performance (reaction conditions: initial SMX, 20.0 mg/L; catalyst, 400 mg/L).

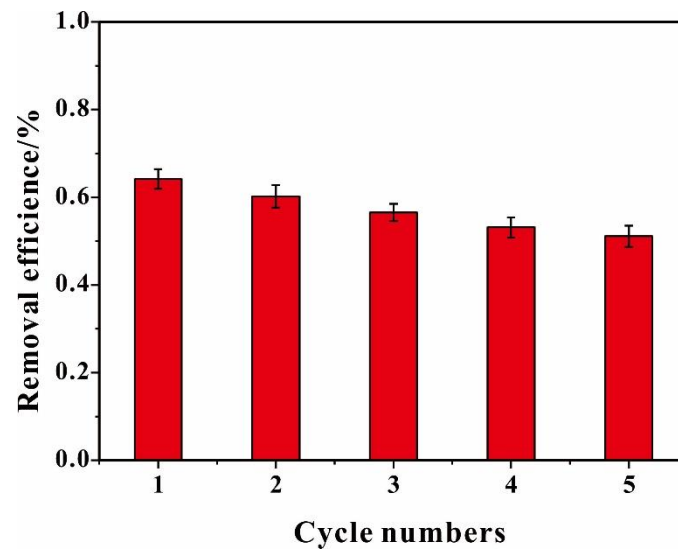


Figure S6. Removal efficiency of TOC (reaction conditions: pH 3.0; initial SMX, 20.0 mg/L; catalyst, 400 mg/L; H₂O₂, 4.0 mM).

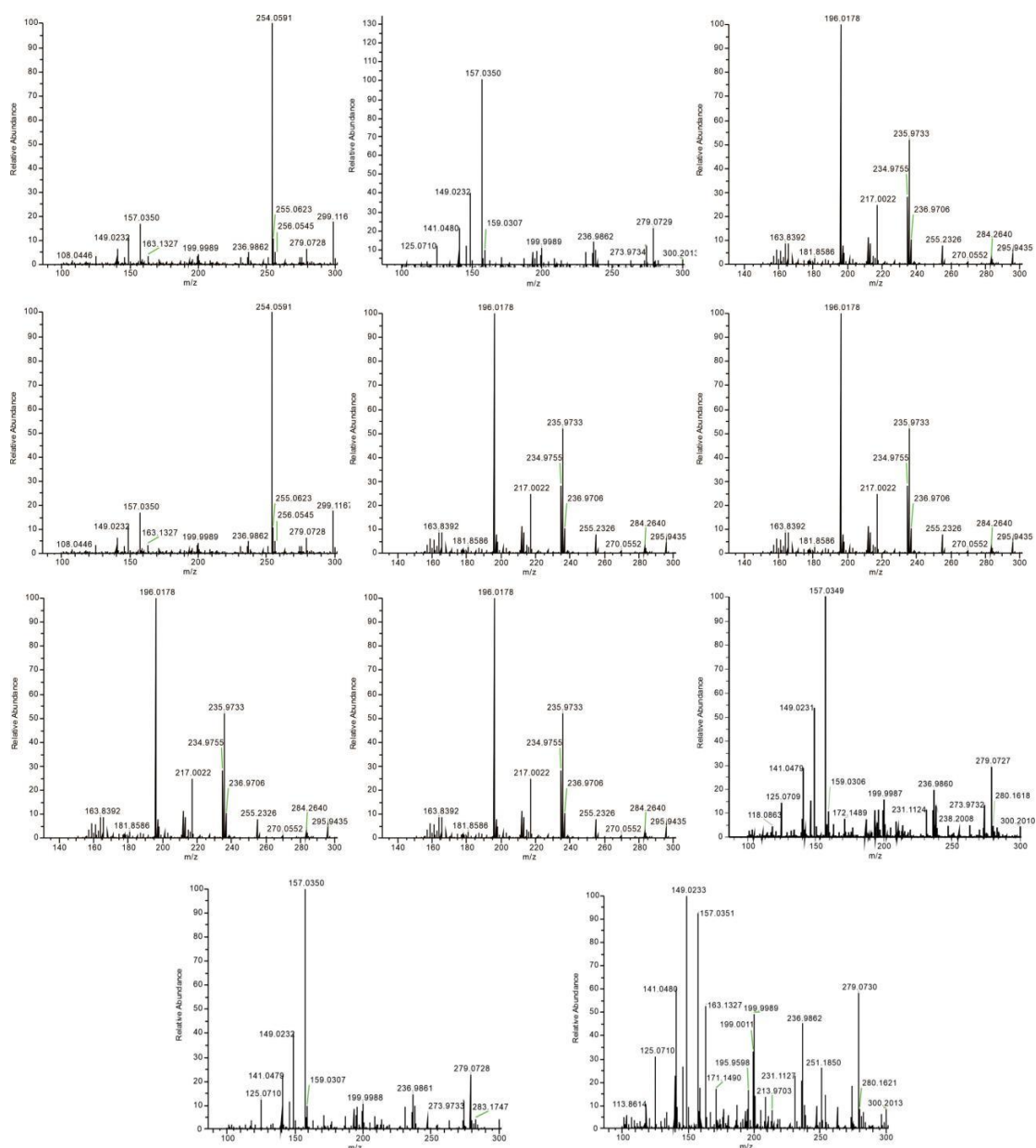
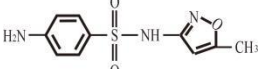
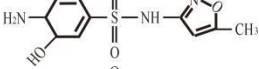
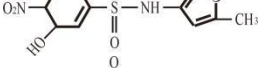
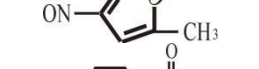


Figure S7. Liquid-mass diagram of SMX and its intermediates in photo-Fenton system.

Table S1. The chemical properties of HO-UIO-66/DE-0, HO-UIO-66/DE-300, HO-UIO-66/DE-400, and HO-UIO-66/DE-500.

| Element | HO-UIO-66 /DE-0 | HO-UIO-66 /DE-300 | HO-UIO-66 /DE-400 | HO-UIO-66 /DE-500 |
|----------------|----------------------------|------------------------------|------------------------------|------------------------------|
| Si | 39.80% | 41.93% | 42.08% | 43.80% |
| O | 39.11% | 37.87% | 37.61% | 36.77% |
| N | 14.18% | 14.03% | 13.85% | 13.28% |
| C | 4.36% | 4.31% | 4.24% | 4.11% |
| Zr | 1.45% | 1.42% | 1.41% | 1.33% |

Table S2. The structural information of the possible intermediate products.

| Compounds | Formula | m/z | Proposed structure |
|-----------|---|-----|---|
| SMX | C ₁₀ H ₁₁ N ₃ O ₃ S | 254 |  |
| SMX 1 | C ₁₀ H ₁₃ N ₃ O ₄ S | 272 |  |
| SMX 2 | C ₁₀ H ₁₁ N ₃ O ₆ S | 299 |  |
| SMX 3 | C ₁₀ H ₉ N ₃ O ₅ S | 284 |  |
| SMX 4 | C ₆ H ₆ N ₂ O ₅ S | 235 |  |
| SMX 5 | C ₆ H ₄ N ₂ O ₄ S | 217 |  |
| SMX 6 | C ₄ H ₆ N ₂ O ₄ S | 181 |  |
| SMX 7 | C ₄ H ₆ N ₂ O ₅ S | 196 |  |
| SMX 8 | C ₄ H ₄ NO ₂ | 113 |  |
| SMX 9 | C ₆ H ₈ N ₂ O ₂ S | 172 |  |
| SMX 10 | C ₆ H ₇ NO ₂ S | 156 |  |